

Conductance Peak Distributions in Quantum Dots and the Crossover between Orthogonal and Unitary Symmetries

Y. Alhassid^{1,2}, J. N. Hormuzdiar¹ and N.D. Whelan³

¹ *Center for Theoretical Physics, Sloane Physics Laboratory, Yale University, New Haven, Connecticut 06520*

² *Institute for Theoretical Physics, University of California, Santa Barbara, California 93106*

³ *Division de Physique Théorique*, Institut de Physique Nucléaire, 91406 Orsay Cedex, France and CATS, Niels Bohr Institute, 17 Blegdamsvej Copenhagen, Denmark*

(November 13, 2018)

Abstract

Closed expressions are derived for the resonance widths and Coulomb blockade conductance peak heights in quantum dots for the crossover regime between conserved and broken time-reversal symmetry. The results hold for leads with any number of possibly correlated and inequivalent channels. Our analytic predictions are in good agreement with simulations of both random matrices and a chaotic billiard with a magnetic flux line.

PACS numbers: 73.40.Gk, 05.45+b, 73.20.Dx, 24.60.-k

Typeset using REVTeX

Recent advances in submicron technology have made it possible to fabricate ballistic quantum dots in which the electron mean free path exceeds the system size. For dots with irregular shapes, the dynamics is largely chaotic [1] and its signatures are observed in the transport properties of the device [2]. In dots that are weakly coupled to external leads via tunnel barriers, the resonances are isolated, and at low temperatures the conductance is dominated by the resonance that is closest to the Fermi energy in the leads. Such closed microstructures thus offer a unique opportunity to probe the chaotic signatures of individual wavefunctions. Since the charging energy of the dot is large compared with the mean-level spacing, the conductance exhibits a series of almost equally spaced peaks versus the gate voltage (Coulomb blockade oscillations). The peaks show order-of-magnitude fluctuations which are explained by a statistical theory [3,4]. The distributions of the conductance peak heights were measured for both conserved and broken time-reversal symmetry [5,6], and were found to agree with theory. Using the supersymmetry technique for disordered systems [7,8] and random matrix theory (RMT) [9], closed expressions for width and conductance peak distributions were derived for any number of possibly correlated channels for both orthogonal and unitary symmetries.

In this letter we derive exact expressions for the universal width and conductance peak distributions in the crossover regime between conserved and broken time-reversal symmetry for any number of possibly correlated and/or inequivalent channels. An approximate expression for the distribution of the wavefunction intensity at a fixed spatial point was obtained in Ref. [10], and an exact expression was derived in Ref. [11] using supersymmetry. The averaged intensity over the complete spectrum of the random matrix was derived in Ref. [12].

At low temperatures $\Gamma \ll kT \ll \Delta$, the conductance peak amplitude G is given by [13] $G = \frac{e^2}{h} \frac{\pi\bar{\Gamma}}{4kT} g$ where

$$g = \frac{2}{\bar{\Gamma}} \frac{\Gamma^l \Gamma^r}{\Gamma^l + \Gamma^r} . \quad (1)$$

Here $\Gamma^{l(r)}$ is the width of a resonance to decay into the left (right) lead and $\bar{\Gamma}$ is the total

average width. g is dimensionless and temperature-independent. In general we assume that the left (right) lead has $\Lambda^{l(r)}$ open channels such that $\Gamma^{l(r)} = \sum_c |\gamma_c^{l(r)}|^2$, where $\gamma_c^{l(r)}$ is the partial amplitude to decay into channel c on the left (right). Using R -matrix theory [3] or resonance theory [14], the partial width amplitude can be expressed in terms of the resonance wavefunction Ψ and the channel wavefunction Φ_c at the lead-dot interface. When each lead is modelled in terms of several point-like contacts \mathbf{r}_c then $\gamma_c \propto \Psi(\mathbf{r}_c)$ [7]. By expanding a resonance wavefunction in a complete basis of solutions $\rho_\mu(\vec{r})$ inside the dot at a fixed energy ($\Psi(\mathbf{r}) = \sum_\mu \psi_\mu \rho_\mu(\mathbf{r})$), the partial width γ_c can be expressed as a scalar product [14] of the vectors that represent the channel and the resonance function $\gamma_c = \langle \phi_c | \psi \rangle \equiv \sum_\mu \phi_{c\mu}^* \psi_\mu$.

In the crossover regime of breaking time-reversal symmetry, the resonance wavefunctions are assumed to have statistical properties which are described by the corresponding eigenvectors ψ of a random matrix ensemble that interpolates between the GOE and GUE [1]

$$H = S + i\alpha A. \quad (2)$$

S and A are, respectively, symmetric and antisymmetric real matrices of dimension N which are uncorrelated and chosen from gaussian ensembles of variance a^2 . The proper transition parameter that describes the crossover from GOE to GUE is given by the ratio of the rms of a typical symmetry-breaking matrix element to the mean-level spacing Δ [15]

$$\lambda = \frac{\alpha a}{\Delta} = \frac{\alpha \sqrt{N}}{\pi}, \quad (3)$$

where we have used the mean level density at the middle of the spectrum. The complete breaking of time-reversal symmetry occurs for $\lambda \sim 1$. Since the transition parameter depends on the level density, we shall study the ensemble's statistics only around the middle of the spectrum. The spectral properties of the transition ensemble (2) were derived in a closed form [16]. Similar spectral correlators were also derived for a single electron in a disordered medium using the supersymmetry method [17]. However, less is known about the eigenvector statistics and, unlike in the GOE and GUE limits, the eigenvalue and eigenvector distributions do not factorize.

An eigenvector component ψ_μ is a complex number, $\psi_\mu = \psi_{\mu R} + i\psi_{\mu I}$, and can be viewed as a two-dimensional vector in the complex plane. Since the eigenvector $\boldsymbol{\psi}$ is determined only up to a phase $e^{i\theta}$, ψ_μ is determined only up to a rotation by an angle θ . This angle is uniquely determined by rotating to a principal frame in which [15,10]

$$\sum_{\mu=1}^N \psi_{\mu R} \psi_{\mu I} = 0 \ ; \ \sum_{\mu} \psi_{\mu I}^2 / \sum_{\mu} \psi_{\mu R}^2 \equiv r^2 \quad (4)$$

with $0 \leq r \leq 1$. The ratio r^2 is invariant under a rotation and is thus independent of the frame. The right inset of Fig. 1 shows the components of a typical eigenvector in the complex plane. Its general shape is that of an ellipsoid whose semi-axes define the principal axes. In the following, $\psi_{\mu R}$ and $\psi_{\mu I}$ will denote exclusively the components of $\boldsymbol{\psi}$ in this principal frame.

Let us consider eigenvectors with a fixed value of r . Under an orthogonal transformation (in the N -dimensional space) the real and imaginary parts of $\boldsymbol{\psi}$ do not mix so that a principal frame remains principal and r^2 is invariant. Since the probability distribution of the ensemble (2) is also invariant under an orthogonal transformation, the conditional probability of finding an eigenvector $\boldsymbol{\psi}$ given its r -value is

$$P(\boldsymbol{\psi}|r) \propto \delta\left(\sum_{\mu} \psi_{\mu R}^2 - \frac{1}{1+r^2}\right) \delta\left(\sum_{\mu} \psi_{\mu I}^2 - \frac{r^2}{1+r^2}\right) \delta\left(\sum_{\mu} \psi_{\mu R} \psi_{\mu I}\right) . \quad (5)$$

The conditional distribution $P(X|r)$ of any quantity X which is a function of the eigenvector $\boldsymbol{\psi}$ can be calculated from (5). The actual distribution $P_\lambda(X)$ at a given value λ of the transition parameter can then be calculated in terms of the distribution $P_\lambda(r)$ of the quantity r (whose explicit form is given below in Eq. (9))

$$P_\lambda(X) = \int_0^1 P_\lambda(r) P(X|r) \equiv \langle P(X|r) \rangle . \quad (6)$$

The conditional joint distribution of the partial width amplitudes $\boldsymbol{\gamma} = (\gamma_1, \gamma_2, \dots, \gamma_\Lambda)$ for Λ real channels $\boldsymbol{\phi}_c$ can be calculated exactly from (5) and $\gamma_c = \langle \boldsymbol{\phi}_c | \boldsymbol{\psi} \rangle$. In the limit $N \rightarrow \infty$ we obtain a Gaussian distribution in γ_{cR} and γ_{cI}

$$P(\boldsymbol{\gamma}|r) \propto \exp\left(\frac{1+r^2}{2} \boldsymbol{\gamma}_R^T M^{-1} \boldsymbol{\gamma}_R + \frac{1+r^2}{2r^2} \boldsymbol{\gamma}_I^T M^{-1} \boldsymbol{\gamma}_I\right) , \quad (7)$$

where $\gamma_c = \gamma_{cR} + i\gamma_{cI} = \langle \phi_c | \psi_R \rangle + i \langle \phi_c | \psi_I \rangle$ is a principal frame decomposition, and γ^T denotes the transpose of the column vector γ . The matrix M is the channel correlation matrix $M_{cc'} = \overline{\gamma_c^* \gamma_{c'}} = \langle \phi_c | \phi_{c'} \rangle$. To calculate M for a chaotic system, we note that the relation $\overline{\psi_\mu^* \psi_{\mu'}} = N^{-1} \delta_{\mu\mu'}$ is valid for the transition ensemble irrespective of the value of λ . We can therefore repeat the derivation of Ref. [9] to find for M an expression identical to the one obtained in either the orthogonal or unitary limits. For point-like contacts $M_{cc'} \propto J_0(k|\mathbf{r}_c - \mathbf{r}'_c|)$, independently of the crossover magnetic field.

As a special case of (7) we obtain the conditional distribution of a single component ψ_μ of an eigenvector by choosing a single channel along the μ -th axis. At a fixed r , $\psi_{\mu R}$ and $\psi_{\mu I}$ are independent Gaussian variables with $\overline{\psi_{\mu I}^2} / \overline{\psi_{\mu R}^2} = r^2$. The full distributions of the real and imaginary parts of the wavefunction amplitude are obtained by a weighted average of the conditional distributions according to Eq. (6) and are not statistically independent. Fig. 1 shows these distributions for $\lambda = 0.1$. A Gaussian distribution (dashed line) is a good approximation for the real part of the wavefunction amplitude, but not for the imaginary part.

The distribution of the width $\Gamma = |\gamma|^2 = \gamma_R^2 + \gamma_I^2$ for a one-channel lead is found to be

$$P_\lambda(\hat{\Gamma}) = \langle a_+ e^{-a_+^2 \hat{\Gamma}} I_0(a_+ a_- \hat{\Gamma}) \rangle, \quad (8)$$

where $\hat{\Gamma} = \Gamma / \bar{\Gamma}$, $a_\pm \equiv (r^{-1} \pm r) / 2$ and I_0 is the modified Bessel function of order zero. An exact expression for the distribution of the wavefunction intensity (at a fixed spatial point) was derived in Ref. [11] through the supersymmetry method. By comparing our result (8) with the result in [11], we find that the r -distribution is given by

$$P_\lambda(r) = \pi^2 \lambda^2 (1/r^3 - r) e^{-\frac{\pi^2}{2} \lambda^2 (r-1/r)^2} \left\{ \phi_1(\lambda) + [(r + 1/r)^2 / 4 - 1/2 \pi^2 \lambda^2] [1 - \phi_1(\lambda)] \right\}, \quad (9)$$

where $\phi_1(\lambda) = \int_0^1 e^{-2\pi^2 \lambda^2 (1-t^2)} dt$. RMT simulations confirm that Eq. (9) is indeed the r -distribution (see left inset in Fig. 1). Eqs. (7), (6) and (9) provide a closed analytic expression for the joint partial amplitudes distribution for a lead with any number of possibly correlated and inequivalent channels.

To derive a closed expression for the total width distribution for multi-channels leads, we note that the conditional distribution $P(\gamma|r)$ in Eq. (7) is identical to a GOE distribution for 2Λ channels with partial amplitudes γ_{cR}, γ_{cI} and a correlation matrix \mathcal{M} composed of four $\Lambda \times \Lambda$ blocks

$$\mathcal{M} = \begin{pmatrix} \frac{1}{1+r^2}M & 0 \\ 0 & \frac{r^2}{1+r^2}M \end{pmatrix}. \quad (10)$$

We can therefore use the known distributions from the GOE limit [9]. The 2Λ eigenvalues of \mathcal{M} are given by $\{\omega_j^2\} = \{\frac{1}{1+r^2}w_c^2, \frac{r^2}{1+r^2}w_c^2\}$ where w_c^2 are the Λ eigenvalues of M . Sorting the inverse eigenvalues of \mathcal{M} in ascending order $\omega_1^{-2} < \omega_2^{-2} < \dots$, we have

$$P_\lambda(\Gamma) = \left\langle \frac{1}{\pi 2^\Lambda} \left(\prod_c \frac{1}{\omega_c} \right) \sum_{m=1}^\Lambda \int_{1/2\omega_{2m-1}^2}^{1/2\omega_{2m}^2} d\tau \frac{e^{-\Gamma\tau}}{\sqrt{\prod_{r=1}^{2m-1} (\tau - \frac{1}{2\omega_r^2}) \prod_{s=2m}^{2\Lambda} (\frac{1}{2\omega_s^2} - \tau)}} \right\rangle. \quad (11)$$

Similarly we can use the closed expression for the GOE conductance distribution [9] to obtain $P(g|r)$ analytically and then use (6) to find $P_\lambda(g) = \langle P(g|r) \rangle$. In this calculation of $P(g|r)$ (where Eq. (1) is exploited), we take advantage of the statistical independence of the conditional distributions of the total widths in the left and right leads, i.e. $P(\Gamma^l, \Gamma^r|r) = P(\Gamma^l|r)P(\Gamma^r|r)$. We note however that the widths themselves are not independent since $\langle P(\Gamma^l|r)P(\Gamma^r|r) \rangle \neq \langle P(\Gamma^l|r) \rangle \langle P(\Gamma^r|r) \rangle$. The distant correlation of wavefunctions in the crossover regime [18] follows from this relation. The universal conductance peaks distributions $P_\lambda(g)$ for one-channel symmetric leads are shown in Fig. 2 for several values of λ in the crossover regime. A good approximation (see left inset in Fig. 2) is $P_\lambda(g) \approx P(g|r_0)$, where $r_0 = r_0(\lambda)$ (see right inset in Fig. 2) is determined by finding the best fit to the exact $P_\lambda(\Gamma)$ for a single channel. r_0 can also be estimated by $\langle r \rangle$ (solid line in the right inset in Fig. 2).

To test our RMT predictions for the crossover conductance distributions, we used the conformal billiard [19] (threaded by an Aharonov-Bohm flux line Φ) whose shape is determined by the image of the unit circle in the complex z -plane under the conformal mapping $w(z) = (z + bz^2 + be^{i\delta}z^3)/\sqrt{1+5b^2}$. We collected statistics from several uncorrelated and fully chaotic billiards with $\delta = \pi/2$ and various values of b . Semiclassical considerations

for weak fields [20] lead to a linear relation $\lambda = \Phi/\Phi_{cr}$. Φ_{cr} is the crossover flux given by $\Phi_{cr}/\Phi_0 = (\pi/4)(\alpha_g^2\mathcal{N})^{-1/4}$, where \mathcal{N} is the number of electrons within the dot and α_g is a geometrical factor. Except for a constant factor, this crossover field has a similar expression to that of the correlation field [14]. Rather than calculating the geometrical factor semiclassically, we determined the exact relation between λ and Φ/Φ_0 by fitting the Dyson-Mehta Δ_3 spectral statistics to its known analytic form [16,20]. The results for the lowest 300 eigenvalues are shown in the top inset in Fig. 3. For each lead we chose a sequence of Λ equally spaced points on the billiard boundary with spacing $|\Delta\mathbf{r}|$. To test our expression for the correlation matrix M , we have calculated the averaged wavefunction amplitude correlations and found them to be in good agreement with $J_0(k|\Delta\mathbf{r}|)$ independent of the flux (see the inset to the middle panel of Fig. 3). Fig. 3 compares the conductance distributions in the conformal billiard with $\Phi/\Phi_0 = 0.04$ (histograms) to the theoretical predictions (using $\lambda = 0.16$ from the inset) for three cases: one-channel leads, two-channel leads with $k|\Delta\mathbf{r}| = 0.5$ and four-channel leads with $k|\Delta\mathbf{r}| = 2.4$. In each case we also show the limiting distributions for conserved and fully broken time-reversal symmetry. The billiard calculations are in good agreement with the intermediate distributions.

In conclusion, we have derived in closed form the width and conductance peak distributions in a chaotic quantum dot for leads with any number of possibly correlated channels in the crossover regime from orthogonal to unitary symmetry. The distributions depend only on the symmetry-breaking transition parameter and the channel correlation matrix M in each lead. This work was supported in part by the DOE, Grant No. DE-FG02-91ER40608 and by the NSF, Grant No. PHY94-07194. NDW was supported by the European Human Capital and Mobility Programme and by NSERC Canada. YA acknowledges useful discussions with S. Tomsovic.

REFERENCES

- * Unité de recherche des Universités de Paris XI et Paris VI associée au CNRS.
- [1] O. Bohigas, in *Chaos and Quantum Physics*, edited by M.-J. Giannoni, A. Voros and J. Zinn-Justin (North-Holland, Amsterdam, 1991).
- [2] *Mesoscopic Quantum Physics*, edited by E. Akkermans, G. Montambaux, J.-L. Pichard and J. Zinn-Justin (North-Holland, Amsterdam, 1995).
- [3] R.A. Jalabert, A.D. Stone, and Y. Alhassid, Phys. Rev. Lett. **68**, 3468 (1992).
- [4] V.N. Prigodin, K.B. Efetov, and S. Iida, Phys. Rev. Lett. **71**, 1230 (1993).
- [5] A.M. Chang, H.U. Baranger, L.N. Pfeiffer, K.W. West and T.Y. Chang, Phys. Rev. Lett. **76**, 1695 (1996).
- [6] J.A. Folk, S.R. Patel, S.F. Godijn, A.G. Huibers, S.M. Cronenwett, C.M. Marcus, K. Campman and A.C. Gossard, Phys. Rev. Lett. **76**, 1699 (1996).
- [7] E.R. Mucciolo, V.N. Prigodin, and B.L. Altshuler, Phys. Rev. B **51**, 1714 (1995).
- [8] V. N. Prigodin, N. Tanigushi, A. Kudrolli, V. Kidambi, and S. Sridhar, Phys. Rev. Lett. **75**, 2392 (1995).
- [9] Y. Alhassid and C.H. Lewenkopf, Phys. Rev. Lett. **75**, 3922 (1995); Los Alamos archives cond-mat/9609080.
- [10] K. Zyczkowski and G. Lenz, Z. Phys. B **82**, 299 (1991).
- [11] V.I. Fal'ko and K.B. Efetov, Phys. Rev. B **50**, 11267 (1994).
- [12] H.-J. Sommers and S. Iida, Phys. Rev. E **49**, R2513 (1994).
- [13] C.W.J. Beenakker, Phys. Rev. B **44**, 1646 (1991).
- [14] Y. Alhassid and H. Attias, Phys. Rev. Lett. **76**, 1711 (1996); Phys. Rev. B **54**, 2696 (1996).

- [15] J.B. French, V.K.B. Kota, A Pandey and S. Tomsovic, Phys. Rev. Lett. **54**, 2313 (1985);
Ann. Phys. (NY) **181**, 198 (1988).
- [16] A. Pandey and M.L. Mehta, Commun. Math. Phys. **87**, 49 (1983); M.L. Mehta and A.
Pandey, J. Phys. A **16** 2655, L601 (1983).
- [17] A. Altland, S. Iida and K.B. Efetov, J. Phys. A **26**, 3545 (1993).
- [18] V.I. Fal'ko and K.B. Efetov, Phys. Rev. Lett. **77**, 912 (1996).
- [19] M.V. Berry and M. Robnik, J. Phys. A **19**, 649 (1986).
- [20] O. Bohigas, M.-J. Giannoni, A. M. Ozório de Almeida, and C. Schmit, Nonlinearity **8**,
203 (1995).

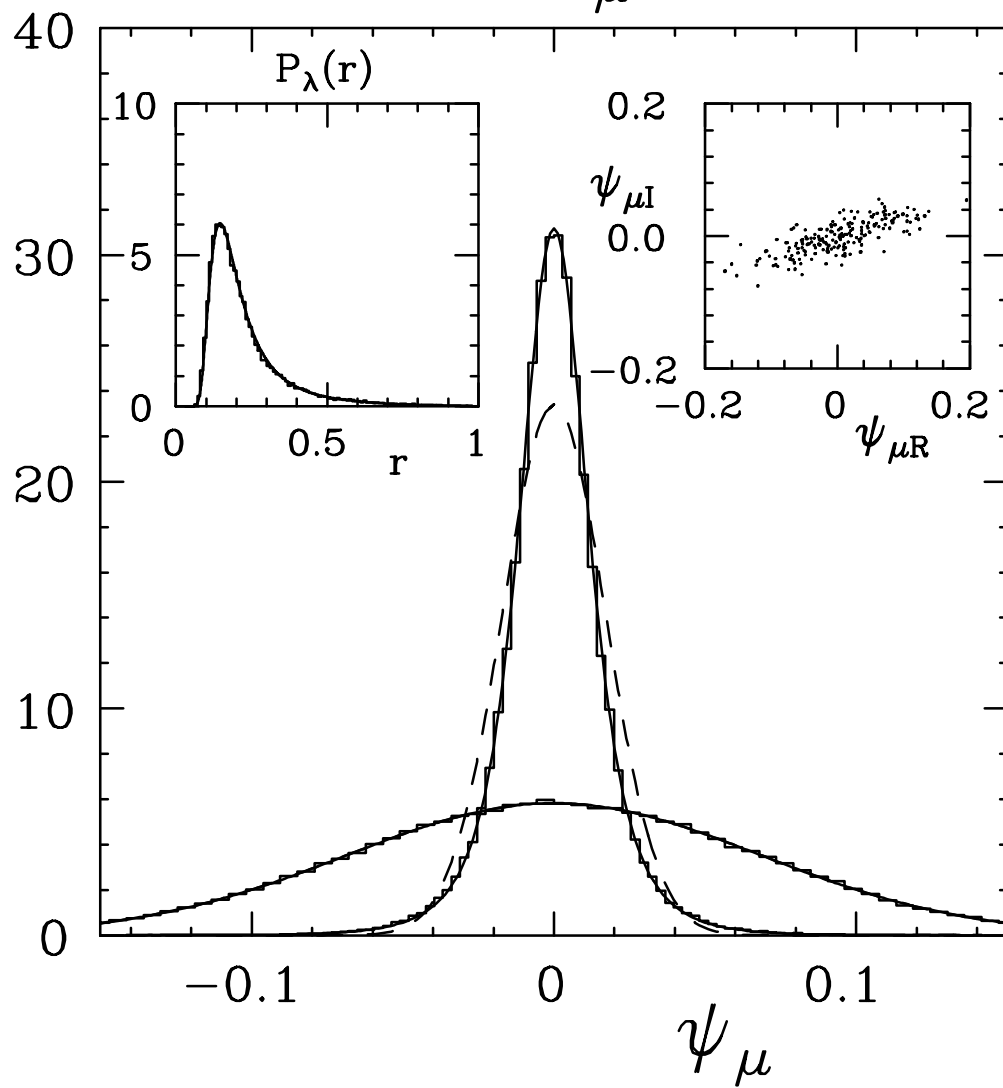
FIGURES

FIG. 1. The distributions $P(\psi_{\mu R})$ (wider) and $P(\psi_{\mu I})$ (narrower) of the real and imaginary parts of an eigenvector component in the principal frame for $\lambda = 0.1$. Histograms: simulations of the RMT ensemble (2); dashed lines: a Gaussian approximation; solid lines: the exact analytic results. The right inset shows the components of a typical vector in the complex amplitude plane. The left inset is the r -distribution $P_\lambda(r)$ for $\lambda = 0.1$, where the solid line is the analytic result (9) and the histogram is from RMT simulations.

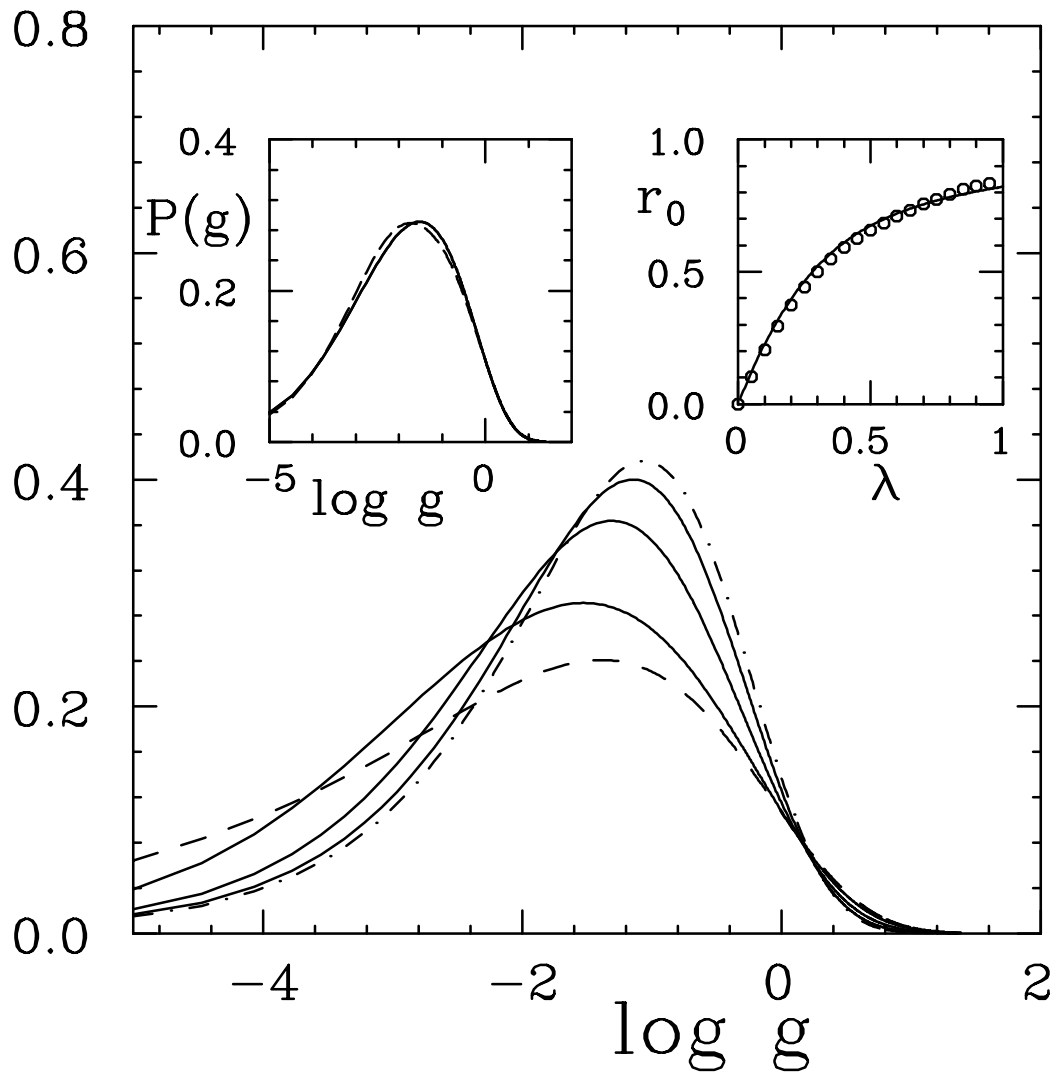
FIG. 2. Conductance peak distributions $P_\lambda(g)$ vs. $\log g$ in the crossover from conserved to broken time-reversal symmetry for one-channel symmetric leads: $\lambda = 0$ (GOE, dashed), 0.1, 0.25, 0.5 (solid lines) and $\lambda \gg 1$ (GUE, dot-dashed). Curve maxima increase with λ . The left inset compares the Gaussian approximation for $P(g)$ (dashed) with the exact result (solid) for $\lambda = 0.1$. Shown in the right inset is $r_0(\lambda)$ (circles) and $\langle r \rangle_\lambda$ versus λ (solid line).

FIG. 3. Conductance peak distributions $P(g)$ in the conformal billiard (histogram) for Λ point-contact symmetric leads and flux of $\Phi/\Phi_0 = 0.04$ for several values of Λ and $k|\Delta\mathbf{r}|$. In each case we show the analytic predictions (solid lines) as well as the GOE (dashed) and GUE (dot-dashed) limits. The top inset describes the transition parameter λ as a function of magnetic flux Φ/Φ_0 . The inset in the middle panel shows the spatial correlations of the eigenfunctions for $\Phi/\Phi_0 = 0.02, 0.06$ and 0.10 (diamonds, pluses and x's, respectively). The solid line is the theoretical prediction.

$$P(\psi_\mu)$$



$P(g)$



$$\Phi/\Phi_0=0.04$$

